Comparison between resonant L_α emission spectra and resonant LMM Auger spectra of yttrium compounds

Shun-ichi Nakai, Takayuki Kashiwakura, Katsuhiro Sasaki and Tohru Watanabe

Department of Electrical and Electronic Engineering, Utsunomiya University, Utsunomiya 321-8585 Japan.
E-mail: nakai@cc.utsunomiya-u.ac.jp

Resonant L_α x-ray emission spectra (RXES) and resonant LMM Auger emission spectra (RAES) of Yttrium compounds were measured across YL_{III} absorption threshold. When the incident photon energy is bellow the absorption threshold, only Raman scattering component is commonly observed in both spectra. Above the absorption threshold, Raman and normal L_α (or normal LMM Auger) emission peaks are observed in insulator samples. These spectral features are almost same in both RXES and RAES processes, except for the relative intensity ratio between these Raman peaks and normal L_α (or normal LMM Auger) emission peaks. Comparing these two spectra, useful information about the deexcitation of core hole can be obtained.

Keywords: resonant x-ray Raman; resonant Auger Raman;

1. Introduction

Resonant x-ray Raman scattering process was predicted theoretically by Noziéres and Abrahams (1974) and was first observed experimentally by Sparks (1974) for the inelastic scattering peak using Cu K_α line from ordinary x-ray tube. Eisenberger *et al.* (1976) studied the resonant x-ray Raman scattering process around the K edge of Cu metal by means of synchrotron radiation. They found that the x-ray Raman scattering peak was resonantly enhanced as the energy of the incident photon was tuned across the K edge. Theoretical discussions for the resonant x-ray Raman scattering process have been given by Tulkki (1983), Åberg and Tulkki (1994). The core-hole states are relaxed also through a radiationless process, the Auger decay process. Brown *et al.* (1980) studied the LMM Auger process for atomic Xe using synchrotron radiation around the L absorption edge. They found Auger peaks which show linear dispersion as a function of incident photon energy and were resonantly enhanced at the strong absorption region. These peaks are assigned to the process which is analogous to the resonant x-ray Raman process, and called the Auger resonant Raman process. Several studies have been carried out on this resonant Raman process during last 10 years. (Elango *et al*., 1993) (Óbrien *et al*., 1993) (Ice *et al*., 1993) (Baba *et al.*, 1994) (MacDonald *et al*., 1995) (Kashiwakura *et al*., 1996) (Tezuka *et al*., 1996)

Recently, we studied the RXES of 4d transition-metal compounds, YF_3, YCl_3, Y_2O_3 and Y-metal across Y L_{III} absorption threshold. (Nakai *et al*., 2000) We observed the resonant Raman component bellow and above the absorption threshold in insulator samples. The Raman scattering component has a two peak structure, main and subpeaks. Theoretically calculated results by Mizouchi (1999) suggested the appearance of two such peaks.

García de Abajo et al. (1999) reported the multiatom resonant photoemission (MARPE). Arenholtz et al. (2000) observed the MARPE via secondary process, Auger decay and x-ray fluorescence. The two processes are competitive, therefore, it is very interesting to investigate such a core hole decay phenomenon through radiative and radiationless processes. By comparing the results obtained from both processes, it is expected that the information about the interaction between an excited electron and an Auger electron or an emitted photon has been obtained.

2. Experiments

The experiments were performed at the double crystal beamline BL-11B of the Photon Factory, IMSS, High-Energy Accelerator Research Organization, Tsukuba. An incident photon energy was selected with Ge(111) monochromator. X-ray absorption spectra (XAS) of Y-metal, YF_3 and YCl_3 were recorded using the total electron yield method. The secondary x-ray emission spectra (XES) were obtained using a monochromator composed of a curved PET(002) crystal and a gas flow proportional counter. The intensity of incident photons was monitored by means of a photocurrent from a Cu mesh that was arranged in front of a sample. The energy resolution of this monochromator was about 1.0 eV for the Y L_α emission line. The Y-metal sample was in a sheet. The samples of YF_3 and YCl_3 were polycrystalline powders and prepared by uniformly rubbing fine powder onto Cu plate. The take off angle of emitted photons was 45° from the sample surface. The Auger spectra were measured with the same double crystal monochromator at the beamline BL-11B. The energy spectra of electrons emitted from the sample were analyzed with a double-pass cylindrical mirror analyzer (DCMA). The total energy resolution of the energy analyzer was about 0.5 eV. Y-metal sample was scraped by a diamond file prior to measurement. Surface oxidation was monitored by measuring photoelectron spectra of O 1s line. YF_3 and YCl_3 samples were prepared *in situ* by evaporation onto Cu substrates. The pressure in the analyzer chamber was about 6.5×10^{-8} Pa during measurement.

3. Results and Discussion

Figure 1(a) shows the L_{III} XAS of YF_3. The main absorption peak at 2083.5 eV is assigned to the Y $2p_{3/2} \rightarrow$ Y $4d_{5/2}$ transition. The RXES were taken at selected excitation energies showed by vertical arrows for 1 to 18 in (a) are represented in Fig.1(b). The intensity of each spectrum is normalized with an incident photon flux. Below the absorption threshold, two peaks (main peak is shown with white arrow, subpeak is shown with vertical bar) are observed. The peak energies of spectra are shift linearly with incident photon energies and the intensity increases as the photon energy approached the absorption edge. These peaks are assigned to the Raman scattering process. In this Raman scattering process, the intermediate states are virtual bound states under the conduction band, then photoexcited electrons enter the conduction band in the final state. Therefore, this optical process is of the second order and then, the peak energy of the Raman spectra changes linearly with the incident photon energy. The energy difference and the intensity ratio of these main and subpeaks are almost constant except for the resonance region. The theoretically calculated results by Mizouchi (1999) suggest the appearance of two such peaks. The main peak comes from R_1 (ω_i, ω_f) term of Raman process in

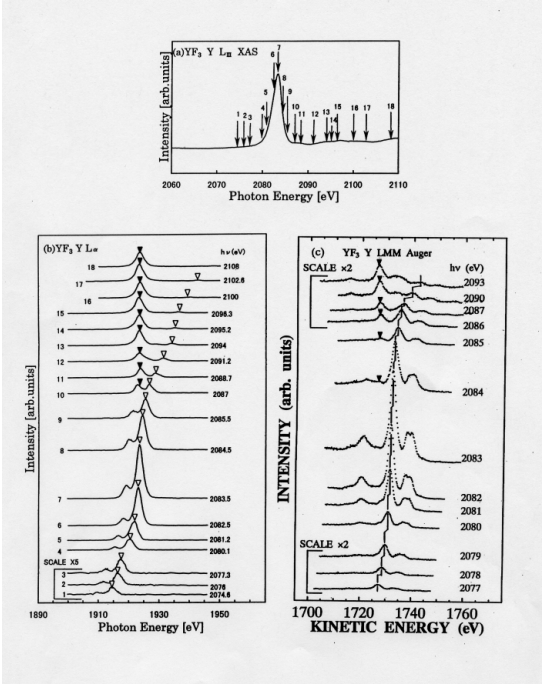

Figure 1
(a) YL_{III} XAS of YF_3, (b) YL_α RXES for YF_3, (c) Y LMM RAES for YF_3, excited with different photon energies, as indicated by arrows in (a). These spectra are reproduced from Ref. (Nakai and Tezuka).

whose final state, only one electron is left in the conduction band at $|f_1>>$. The subpeak is due to the off-resonant process of R_2 (ω_i, ω_f) in whose final state, a conduction-electron-valence -hole pair as well as a conduction electron is left at $|f_2>>$. Above the absorption edge, the Raman peaks and the normal L_α emission peaks (the peak positions are shown with black arrows) are observed. As the incident photon energy becomes larger, the intensity of the normal L_α emission peak shows almost constant, while that of the Raman peak becomes smaller and disappears at about 20 eV above the absorption peak.

The Y LMM resonant Auger spectra of YF_3 taken at selected excitation energies indicated by vertical arrows in (a) are shown in Fig.1 (c). The intensity of each spectrum is normalized relative to the F 1s core spectrum. The resonant Auger Raman peaks (the main peak is shown with vertical bar) are observed across the L_{III} absorption edge. This Auger Raman process is analogous to the resonant Raman scattering process observed in L_α emission spectra. However, subpeak which is clearly observed in Raman component of RXES is not observed, because Auger Raman peaks are composed of three peaks which are assigned to multiplet terms of final-state, then the subpeak may be smeared out. Above the absorption peak, normal Auger peak (the peak position is shown with black arrow) is also observed, however, the peak intensities are low. These spectral features are almost same as that of RXES except for the relative intensity.

In order to compare the RXES with the RAES, we decompose the spectra into Raman and normal L_α emission peaks (or Auger Raman and normal LMM Auger peaks). The intensities and peak positions of the RXES and the RAES are plotted as a function of incident photon energy in Fig. 2~4 for YF_3, YCl_3

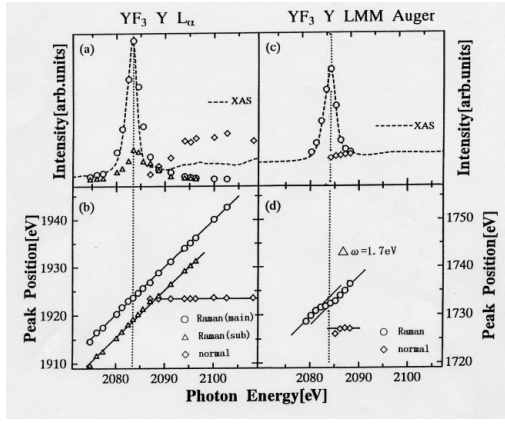

Figure 2
Peak intensities (a) and positions (b) of RXES for YF_3 as a function of incident photon energy. Peak intensities (c) and positions (d) of RAES for YF_3. The dotted vertical lines show the position of the L_{III} absorption peak. $\Delta\omega$ represents the fixed photon energy region, irrespective of the incident photon energy.

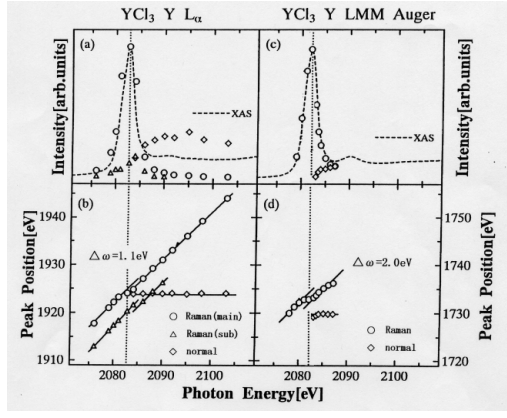

Figure 3
Peak intensities (a) and positions (b) of RXES for YCl_3 as a function of incident photon energy. Peak intensities (c) and positions (d) of RAES for Y Cl_3.

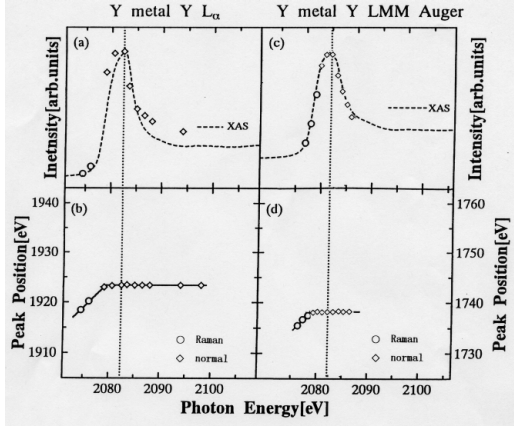

Figure 4
Peak intensities (a) and positions (b) of RXES for Y-metal as a function of incident photon energy. Peak intensities (c) and positions (d) of RAES for Y-metal.

and Y-metal, respectively. The peak position and intensity are estimated by line shape analysis of the spectra. In this line shape analysis, line shape at the off-resonant region was assumed as a natural line shape and was assumed to be a Lorentzian convoluted with a Gaussian. A peak narrowing effect as observed in the resonant Cu 1s excitation is also expected, however, we didn't take into account such a narrowing effect for our line shape analysis. In Fig. 2(a), the integrated intensities of main Raman peak (circles), sub-Raman peak (triangles) and normal L_α emission peak (diamonds) are plotted as a function of incident photon energy. The dashed line shows a XAS curve whose maximum intensity is normalized to that of the main Raman peak. As seen in Fig. 2(a), the resonant enhancement is observed in both main and sub-Raman peaks and corresponds well to the XAS. The peak positions of these three peaks are plotted in Fig. 2(b) as a function of incident photon energy. The Raman peak shifts linearly with increasing incident photon energy across the absorption threshold. The dotted vertical line in Fig. 2(a) and 2(b) shows the position of the L_{III} absorption peak. Figure 2(c) and 2(d) also show the RAES of YF_3. The peak positions of Raman peaks of RXES (Fig. 2(b)) show linear dependence as incident photon energy increases below and above the absorption threshold. On the other hand, in RAES (Fig. 2(d)), the peak positions of Auger Raman peaks are fixed in the strong absorption region, irrespective of the incident photon energy. This fixed photon energy region $\Delta\omega$ is shown in Fig. 2(d), ($\Delta\omega$ = 1. 7eV for YF_3). Figure 3(a), (b) and (c), (d) show the L_α RXES and LMM RAES for YCl_3. As seen in Fig 3 (a), (b), similar two components as YF_3 are observed in the RXES for YCl_3. For YCl_3, the fixed photon energy region $\Delta\omega$ at the absorption region is estimated to be $\Delta\omega$ = 1.1eV and 2.0eV for RXES (Fig.3(b)) and RAES (Fig.3(d)), respectively. Figure 4(a), (b) and (c), (d) show the L_α RXES and LMM RAES for Y-metal. Above the absorption threshold, no Raman spectrum is observed and only normal L_α emission and normal LMM Auger spectra are observed in both spectra.

From these results, the comparisons between RXES and RAES are summarized as follows.

(1) The resonant Raman peaks are commonly observed below and above the absorption edge in both RXES and RAES for insulator samples, YF_3 and YCl_3.

(2) At the strong absorption region, the energies of these Raman peaks are fixed, irrespective of the incident photon energy. This fixed photon energy region $\Delta\omega$ in RAES is about 2 times larger than that in RXES for YCl_3.

(3) As seen from Fig. 1, the relative intensity ratio between the Raman line at the absorption peak at $h\upsilon$ = 2083.5eV and normal L_α emission line (or normal LMM Auger line) at $h\upsilon$ = 2100eV is about 3 times larger in RAES than RXES.

(4) In metal, the spectral feature is almost same in both RXES and RAES.

The results in (1) and (4) suggest that the character of the RAES is similar to that of the RXES. After forming a particular core hole in the intermediate state, the decay processes: Auger decay and x-ray fluorescence decay processes result from filling a core hole. Therefore, these results can be reasonably accepted.

Arenholtz *et al*. (2000) observed MARPE for Fe_2O_3 and MnO via secondary processes: Auger decay and x-ray fluorescence. The O KLL Auger intensity clearly shows enhancement at the Fe $L_{2,3}$ absorption edge. On the other hand, the O K_α intensity shows minima when the excitation energy is tuned to the Mn $L_{2,3}$ absorption edge instead of the maxima that might be expected based on the simplest interpretation of MARPE. They interpreted that these minima are due to well-known self absorption phenomena of sample for both the excitation and emitted fluorescence intensity. After correction of such self absorption effect, O K_α fluorescence radiation is enhanced at the Mn $L_{2,3}$ edge. Therefore, this difference has its origin in the different probing depth of photoelectrons and fluorescent x-rays. The self absorption effect is also expected in Y L_α emission, therefore, the difference mentioned in (3) can be attributed to the different probing depth of Auger electrons and emission x-rays.

Finally, we discuss the difference mentioned in (2). From our previous experiments, it is concluded that the constant energy region $\Delta\omega$ is related to the width of absorption peak. The absorption peak is assigned to the transition from a 2p core level to the empty 4d states, then this excited electron is relaxed in these states and dissipated. Therefore, the energy of Raman peak is fixed in this absorption region. There are two holes in the final state of Auger decay process, while only one hole is left in the final state of x-ray emission process. Therefore, this difference of $\Delta\omega$ between RXES and RAES may be due to the final state effect of the deexcitation.

This work was supported by a Grant in Aid for Scientific Research (Grant No. 10554012 and No. 11650003) from the Ministry of Education, Science, Sports and Culture, Japan.

References

Åberg, T., and Graseman, B. (1994) *Resonant Anomalous x-ray Scattering*, edited by G. Materlik, C. J. Sparks, and K. Fisher, 431-448, Amsterdam; North-Holland.

Arenholz, E., Kay, A. W. Fadley, C. S., Grush, M. M., Callcott, T. A., Ederer, D. L., Heske, C. and Hussain, Z. (2000) *Phys. Rev.* B**61**, 7183-7186

Baba, Y, Sasaki, T. A. and Yamamoto, H. (1994) *Phys. Rev*. B**49**, 709-711

Brown, G. S., Chen, M. H., Crasemann, B., and Ice, G. E. (1980) *Phys. Rev. Lett.* **45**, 1937-1940

Eisenberger, P., Platzman, P., M and Winik, H. (1976), *Phys. Rev. Lett*. **36**, 623-626

Elango, M., Ausmees, A., Kikas, A., Nommiste, E., Ruus, R., Saar, A., van Acker, J. F., Andersen, J. N. Nyholm, R. and Martinson, I., (1993) *Phys. Rev.* B**47**, 11736-11748

García de Abajo, F. J., Fadley, C. S. and Van Hove, M. A. (1999) Phys. *Rev. Lett.* **82**, 4126-4129

Kashiwakura, T. Arai, H., Kozuka, N., Odagawa, K., Yokohama, T., Kamata, A. and Nakai, S. (1996) *J. Electron Spectrosc. Relat. Phenom.* **79**, 207-210

MacDonald, M. A,. Southworth, S. H., Levin, J. C., Henins, A,. Deslattes, R. D., LeBrun, T,. Azuma, Y., Cowan, P. L. and Karlin, B. A. (1995) *Phys. Rev.* A**51**, 3598-3603

Mizouchi, H. (1998) *Phys. Rev.* B**58**, 15557-15564

Nakai, S., Megawa, Y., Terasaki, F., Gang Chen, Ohuchi, T., Obara, K., Kojima, T., Arai, H., Kashiwakura, T. and Kitajima, Y. (2000) *Phys. Rev.* B**61**, 7433-7439

Noziéres, E., and Abrahams, E. (1974), *Phys. Rev.* B**10**, 3099-3112

Óbrien, W.L. Jia, J., Dong, Q-Y., Callcott, T.A., Miyano, K. E., Ederer, D. L., Mueller, D. R. and Kao, C-C. (1993) *Phys. Rev. Lett.* **70**, 238-241

Sasaki, T. A., Yoshii, K. Yamamoto, H. and Nakatani, T. (1994) *Phys. Rev.* B**50**, 15519-15526

Sparks, Jr. C. J. (1974) *Phys. Rev. Lett.* **33**, 262-265

Tezuka, H., Arai, H., Kashiwakura, T., Kozuka, N., Yokohama, T., Kamata, A., Nakai, S. and Kitajima, Y., (1996) *J. Electron Spectrosc. Relt. Phenom.* **78**, 123-126

Tulkki, J., *Phys. Rev.* (1983) A**27**, 3375-3377